Bioactive Materials 29 (2023) 265–278

Contents lists available at ScienceDirect

Bioactive Materials

journal homepage: www.keaipublishing.com/en/journals/bioactive-materials

Preclinical evaluation of the safety and effectiveness of a new bioartificial cornea

Yansha Hao [a,b,c,1], Jingting Zhou [a,b,c,1], Ju Tan [a,b,c,1], Feng Xiang [a,b,c], Zhongliang Qin [a,b,c,f], Jun Yao [e], Gang Li [a,b,c], Mingcan Yang [a,b,c], Lingqin Zeng [a,b,c], Wen Zeng [d,**], Chuhong Zhu [a,b,c,*]

[a] Department of Anatomy, Engineering Research Center for Organ Intelligent Biological Manufacturing of Chongqing, key Lab for Biomechanics and Tissue Engineering of Chongqing, Third Military Medical University, Chongqing, 400038, China
[b] Engineering Research Center of Tissue and Organ Regeneration and Manufacturing, Ministry of Education, Chongqing, 400038, China
[c] State Key Laboratory of Trauma, Burnand Combined Injury, Chongqing, China
[d] Department of Cell Biology, Third Military Army Medical University, Chongqing, 400038, China
[e] Hong Chang Biotechnology Co., Ltd, Guangzhou, 510700, China
[f] Zhong Zhi Yi Gu Research Institute, Chongqing Jiukang Medical Research Institute Co., Ltd.,. China

ARTICLE INFO

Keywords:
Decellularization
Bioartificial cornea
Cross-linking
Biocompatibility
Transparency

ABSTRACT

Cross-linking agents are frequently used to restore corneal properties after decellularization, and it is especially important to select an appropriate method to avoid excessive cross-linking. In addition, how to promote wound healing and how to improve scar formation require further investigation. To ensure the safety and efficacy of animal-derived products, we designed bioartificial corneas (BACs) according to the criteria for Class III medical devices. Our BACs do not require cross-linking agents and increase mechanical strength via self-cross-linking of aldehyde-modified hyaluronic acid (AHA) and carboxymethyl chitosan (CMC) on the surface of decellularized porcine corneas (DPCs). The results showed that the BACs had good biocompatibility and transparency, and the modification enhanced their antibacterial and anti-inflammatory properties in vitro. Preclinical animal studies showed that the BACs can rapidly regenerate the epithelium and restore vision within a month. After 3 months, the BACs were gradually filled with epithelial, stromal, and neuronal cells, and after 6 months, their transparency and histology were almost normal. In addition, side effects such as corneal neovascularization, conjunctival hyperemia, and ciliary body hyperemia rarely occur in vivo. Therefore, these BACs show promise for clinical application for the treatment of infectious corneal ulcers and as a temporary covering for corneal perforations to achieve the more time.

1. Introduction

Corneal disease is a major cause of blindness worldwide, second only to cataract in overall importance [1]. The epidemiology of corneal blindness is complicated and includes a wide variety of infectious and inflammatory eye diseases that cause corneal scarring, which leads to functional blindness [2]. Three elements are important for addressing corneal blindness: prevention, treatment, and rehabilitation. When preventive strategies have failed, corneal transplantation is the most effective treatment for advanced corneal disease [3]. However, the global availability of donor corneas is limited, and rejection and graft failure may occur, as with the transplanted of other organs. Thus, there is a need for viable alternatives to donor corneas to increase supply, reduce rejection, and minimize variations in tissue quality [4].

Corneal tissue engineering and regenerative medicine approaches represent a paradigm shift in medical treatment to surmount the shortcomings of current corneal transplantation approaches, mainly immune rejection, limited availability of donor corneas, and the intrinsic regenerative capacity of corneal cells and layers [5]. In recent years, the most widely used tissue scaffold in tissue engineering related to cornea research has been the acellular corneal stroma. However, reconstructing the complex structure, mechanical strength and

Peer review under responsibility of KeAi Communications Co., Ltd.
* Corresponding author.
** Corresponding author.
E-mail addresses: zengw0105@163.com (W. Zeng), zhuch99@tmmu.edu.cn (C. Zhu).
[1] These authors contributed equally.

https://doi.org/10.1016/j.bioactmat.2023.07.005
Received 14 February 2023; Received in revised form 3 July 2023; Accepted 5 July 2023

transparency of the corneal stroma is challenging [6], and research is underway to investigate the functional corneal stroma [7]. In a previous study comparing decellularized materials from 13 animals, including dogs, cats, sheep, goats, cattle, horses and rabbits, pig corneas were found to have the highest similarity to human corneas [8]. The ultimate goal of decellularization is to remove cellular components and genetic materials (e.g., DNA) from native cells while preserving the structural, biochemical, and biomechanical properties of the tissue [9]. There are many methods to decellularize tissues, and most of these methods, including the use of sodium dodecyl sulfate (SDS), salts, 3-[(3-cholamidopropyl)-dimethylammonio]-propanesulf (CHAPS), enzymes such as trypsin and TrypLE Express, NaOH with dispase, and hydrostatic pressure, have been applied to decellularize corneas [10]. These methods often involve the use of nucleases to remove cellular material such as DNA and RNA to reduce the chance of immune rejection, followed by a glycerin soak to restore the clarity of the cornea after decellularization [4].

It is difficult to obtain optimal corneal transplantation results with only one or two acellular procedures [9]. Therefore, recent studies have combined multiple approaches to preserve tissue integrity and ECM structure while achieving maximum removal of cellular components [11]. IImportantly, some human immunogenic epitopes, such as N-glycolylneuraminic acid (Neu5Gc) and galactose-alpha-1,3-galactose (α-Gal), are present in the porcine cornea [12]. The key to successful corneal xenotransplantation is preserving the mechanical and optical properties of the intact cornea and reduce the antigenicity of the corneal components that activate the host immune response [13]. This emphasizes the need for complete decellularization to avoid graft rejection in preclinical applications, but such approaches inevitably destroy the collagenous structure of the decellularized matrix, resulting in poor mechanical properties.

In addition, the corneal epithelium is an integral part of the ocular surface and is necessary to maintain corneal clarity and normal function; when the cornea is damaged, rapid cellular regeneration is important for corneal wound healing [14]. The three-dimensional structure of hydrogels and their water absorption and cytocompatibility make them a favorable choice for scientists to reconstruct damaged corneal tissue [15]. Carboxymethylcellulose (CMC) is the most commonly used polymeric viscosity agent and binds to and is retained by corneal epithelial cells. It increases the viscosity and clearance time of eye drops; additionally, it can stimulate the migration of epithelial cells by binding to matrix proteins, thus effectively reducing the incidence of epithelial cell defects [16]. Hyaluronic acid (HA) is a naturally occurring glycosaminoglycan (GAG) in the extracellular matrix that plays an important roles in development, wound healing, and inflammation [17]. Recent experiments have shown that sodium hyaluronate promotes the migration of human corneal epithelial cells (HCECs) and leads to rapid wound closure through rapid cell migration [18], which is beneficial for corneal wound healing [19]. However, because it lacks the scaffold structure of hyaluronic acid, sodium hyaluronate is easily dissolved in, is absorbed quickly, and persists for only a short time [20]. Due to its poor adhesion and weak mechanical strength, sodium hyaluronate must be chemically modified to obtain more stable biomaterials.

To find a more suitable decellularization and cross-linking procedure to improve the insufficient decellularization of the corneal stroma, in this study, we used low-concentration SDS combined with CHAPS solution and a nonspecific nuclease to completely remove cellular components. In addition, the transparency of the graft was restored by glycerol dehydration, and the inactivation of viruses and pyrogens was achieved via Co60 irradiation and acid–base treatment. Finally, we self-crosslinked porous hydrogels on acellular matrices to improve the biocompatibility of corneal grafts. The need to improve the mechanical properties of bioartificial corneas (BACs) and endow them with anti-inflammatory and antibacterial effects is addressed without using a cross-linking agent. In animal studies, the developed BACs not only induce host cell migration and achieve rapid recellularization of grafts but also promote limbal cell expansion and epithelial cell growth, promoting epithelial cell repair.

2. Materials and methods

2.1. Manufacturing of BACs

BACs are Class III medical devices, and they were manufactured following the principles of good manufacturing practices (GMP) in a Class 4 (according to ISO-14644-1) air quality laminar flow clean-room facility. Although BACs are subjected to an end-stage sterilization process, substantial efforts are made throughout the manufacturing process to maintain the raw materials, intermediate products and final product as aseptically as possible.

In brief, the fabrication procedure was as follows: fresh pig eyeballs were removed within 2 h after death (6- to 7-month-old adult pigs, Zhaolong farm, Chongqing, China). For pretreatment, and the removed pig eyeballs were soaked in 10% hypertonic saline after washing in normal saline three times. Then, they were transported at low temperature (0–4 °C) to the GMP workshop and stored in a −80 °C freezer. Next, corneal slices were prepared. After thawing, the eyeballs were excised and cut into slices with a thickness of 300 μm (for small animal experiments) or 450 μm (for large animal experiments) and a diameter of 9 mm using an automatic microkeratome (Evolution 3e, MORIA S. A, France); high-quality corneal slices with good light transmittance were screened by using a light transmissometer (LS183, Linshang Technology, Shenzhen). These corneas were natural pig corneal (NPC) tissues that were used as controls. Next, the acellular corneal stroma was prepared. Heat removal was achieved by soaking in 1 M hydroxide solution for 30 min at room temperature, followed by washing in PBS solution (3 min × 3 times) and water for injection (WFI) (10 min × 15 times). For the decellularization process, corneal slices were added to 8 mM Chaps solution (0465, Amresco, China) and reacted for 14 h (37 °C, 220 rpm). After washing 3 times with PBS solution, corneal slices were added to 1.8 mM SDS solution (A100227, Sangon Biotech, China) and reacted for 14 h (37 °C, 220 rpm). After washing 16 times with PBS solution, antigen removal was performed. Corneal slices were incubated for 1 h with 5 KU/mL nonspecific nuclease (RPE002, 7Sea Biotech, China) and washed 16 times to remove residual reagent. The above corneas were the decellularized pig cornea (DPC) tissues used as controls. Next, surface modification of corneal slices was performed. First, DPCs were immersed in 0.625 mg/mL aldehyde-modified hyaluronic acid (AHA, 100 kDa, DS ≥ 90%, TS042402, Tanshtech) for 6 h. Amino groups on the surface of the DPCs could be spontaneously cross-linked with hyaluronic acid containing aldehyde groups. Then, DPCs-AHA were immersed in 0.625 mg/mL carboxymethyl chitosan (CMC, 100 kDa, DS ≥ 85%, Aoxing, Zhejiang, China) and incubated for 18 h. The above corneas were the BAC tissues used in the experimental groups. The last steps were dehydration and packaging. The BACs were placed into a bottle with 100 ml pure glycerin and dehydrated for 8 h at 4 °C. Finally, the virus inactivation process involved sterilization of the cornea with an electron accelerator at a dose of 25 kGy.

2.2. Histological examination and scanning electron microscopy

NPCs, DPCs and BACs were embedded in paraffin or O·C.T. compound. The 5 μm sections were stained with hematoxylin-eosin (H&E) and analyzed with an optical microscope (BX 50, Olympus, China). The corneas were fixed with 2.5% glutaraldehyde for 4 h at 4 °C and rinsed in distilled water. The corneas were dehydrated in graded ethanol (50%, 70% 90%, and 100%) and dried with hexamethyldisilazane overnight. The specimens were mounted on stubs and sputter-coated with gold. Images of the lamellar structure of the corneal stroma were obtained using SEM (Crossbeam 340, Zeiss, Germany) at an accelerating voltage of 2 kV.

2.3. DNA, α-Gal, Neu5Gc, collagen, and GAG content analysis

Native pig corneas (NPCs) and BACs were weighed to measure the contents of DNA, α-galactosidase (α-gal), N-glycolylneuraminic acid (Neu5Gc), collagen and glycosaminoglycans (GAGs). Each condition was assessed using 5 samples, and the results were obtained with a microplate reader (Infinite M200, TECAN, Austria).

For the quantification of DNA content, the corneas were digested with proteinase K at 56 °C for 2 h. Genomic DNA was extracted and purified according to the TIANamp Genomic DNA Kit (DP304, TianGen, Beijing, China).

For α-gal analysis, the corneas were processed in lysis solution supplemented with protease inhibitors. After centrifugation, the supernatants were harvested for α-gal quantification via the competitive ELISA method according to the manufacturer's instructions (JM10196P1, JingMei, Jiangsu, China). The α-gal content was quantified against a porcine α-gal standard curve.

For Neu5Gc analysis, corneal tissue was suspended in 1 mL of saline using an automatic sample freeze grinder (JXQECL, Jingxin, Shanghai, China). After centrifugation, the supernatants were harvested for Neu5Gc quantification via the competitive ELISA method according to the manufacturer's instructions (BS-E15064O1, JSBOSSEN, Jiangsu, China). The Neu5Gc content was quantified against a porcine Neu5Gc standard curve.

For collagen analysis, hydroxyproline content was evaluated using the Hydroxyproline Assay Kit (BC0250, Solarbio, Beijing, China). The corneal samples were crushed, added to the extraction buffer, reacted in a 110 °C oven for 2–6 h until digestion was complete, centrifuged at 16,000 rpm, and centrifuged for 20 min. The supernatant was collected for analysis. Each sample was read on a microplate reader at 550 nm. Collagen standards were utilized to calculate the hydroxyproline content.

For glycosaminoglycan (GAG) analysis, the corneas were homogenized and sonicated in PBS supplemented with protease inhibitors on ice. The homogenates were centrifuged, and supernatants were collected for GAG quantification according to the manufacturer's instructions for the Porcine Glycosaminoglycan ELISA Kit (JM10104P2, JingMei, Jiangsu, China).

2.4. Macroscopic transparency and light transmittance

For visual assessment of transparency, corneas were photographed and drawn on white paper with a ruler. The cornea was attached directly to the sample chamber, and a light transmissometer (LS183, Linshang Technology, Shenzhen, China) was used to measure the UV peak wavelength at 365 nm. The infrared peak wavelength was measured at 940 nm; the visible light resonance wavelength was measured at 380–760 nm.

2.5. Mechanical testing

The mechanical properties of the corneas were investigated using a structural universal testing machine (RGM, Reger, Shenzhen, China). BACs were rehydrated in saline for 10–15 min, and NPC tissues were used as controls. A 3 mm × 7 mm cornea was clamped with a 3 mm clip distance for RGM testing (tensile force), and the test speed was 10 mm/min. Each condition was assessed using 5 samples, and the results were plotted as stress–strain curves with GraphPad Prism 9.0 software.

2.6. Swelling analysis

Dry corneas were trimmed into a rectangular shape, and M_1 values were obtained by weighing the samples. Then, the corneas were immersed in normal saline for 24 h. After removal of the corneas from the normal saline, surface moisture was removed; length, width and thickness were measured; and volume V and weight M_2 were calculated. The swelling ratio was calculated according to the following formula: swelling ratio $= (M_2 - M_1)/\rho V$.

2.7. Hyaluronic acid content

The corneal tissues were suspended in 1 mL saline using an automatic sample freeze grinder (JXQECL, Jingxin, Shanghai, China). The corneas were degraded with 100 U/mL hyaluronidase and released hyaluronic acid molecules. The reaction was performed at 37 °C for 24 h in a thermostatic incubator. When the reaction was complete, the supernatant was collected by centrifugation, and the hyaluronic acid content was determined with a Hyaluronic Acid ELISA Kit (EK12338, SAB, USA).

2.8. Anti-inflammatory and antibacterial tests

RAW 264.7 macrophages were plated in 24-well plates at a density of 1×10^5 cells/well and cultured in a 5% CO_2 incubator at 37 °C for 24 h. Thereafter, DPCs and BACs were added to each well and incubated for another 24 h, followed by a challenge with 1 μg/mL lipopolysaccharide (LPS) for 24 h. The supernatant from each well was collected, and the nitrite level was measured using the Griess reaction assay; the levels of tumor necrosis factor-α (TNF-α) and interleukin-1 (IL-1β) were determined using an ELISA kit (Neobioscience, Shenzhen, China). Then, the residual cells were fixed with 4% paraformaldehyde and then subjected to immunofluorescence staining for TNF-α (ab300093, Abcam, 1:100), a marker of macrophage M_1 polarization, and CD11b (ab8878, Abcam, 1:50), a marker of macrophages. Immunofluorescence staining was observed by using a confocal quantitative image cytometer (CQ1, YOKOGAMA, Japan). The antimicrobial activity of BACs against *E. coli* and *S. aureus* was assessed by the plate counting method. The BACs and DPCs were soaked in the bacterial suspension (≈1×10^6 CFU/mL, 1 mL) and incubated for 24 h at 37 °C. Then, 100 μL of bacterial suspension was spread on an agar plate to observe the growth of bacterial colonies. Then, the antimicrobial activity of BACs was determined, with DPCs being used as controls.

2.9. Transplantation of bioartificial corneas

Healthy New Zealand white rabbits (thickness: 300 μm) (3 months, 2.5–3.5 kg, Unisex) were utilized in this study ($n \geq 20$). Healthy beagles (thickness: 450 μm) (3 months, 15–20 kg, Unisex) were used in this study ($n \geq 20$). Healthy primates (thickness: 450 μm) (3 years, 8–12 kg, Unisex) were used in this study ($n \geq 5$). The recipients were anesthetized with an intravenous injection of 10 mg/kg chlorpromazine hydrochloride and 50 mg/kg ketamine hydrochloride diluted in saline. A circular incision was made according to the range of keratoplasty, and a 7~7.5 mm ring drill was generally used for the implant beds. Generally, a diamond 0.25 mm smaller than the graft was used to drill the bed and cut the diseased cornea. The BACs were removed, placed in clean culture dishes, covered with normal saline and removed after 10 min. The corneal endothelium was placed face up on the cutting surface, and the corneal graft was pressed down with sharp pressure from the diamond. The grafts were fixed into the recipient bed via 16 interrupted stitches with 10–0 nylon sutures.

2.10. Postoperative drug administration

According to the guidelines of The Ethics Committee of the Army Military Medical University, after surgery, tobramycin eye ointment was administered three times daily for the first three days. During the epithelial healing period within 2 weeks after surgery, levofloxacin eye drops were administered twice a day, sodium vitrate eye drops were administered three times a day, and tobramycin eye cream was administered once a night. In addition, suture removal was performed for all animals on day 14. Sodium vitrate eye drops, sodium diclofenac

and dexamethasone eye drops were added three times a day within 1 month after surgery. Sodium vitrate eye drops, cyclosporin and dexamethasone eye drops were added three times a day within 3 months after surgery. The graft was fitted after 90 days, and only sodium vitrate eye drops were required three times a day.

2.11. Observation and evaluation of animals in vivo

After transplantation, the animals were closely observed and monitored, and regular slit lamp (SL, 3G, TOPCON, Japan) examination, optical coherence tomography (OCT, HS100, Canon, Japan) and fluorescein staining were performed to assess the degree of corneal edema, the corneal epithelium, corneal transparency, corneal neovascularization, conjunctival congestion, and ciliary congestion. Epithelia, nerve production, the stromal layer, and endothelial cells were monitored by in vivo confocal microscopy analysis of the cornea (HRT3-RCM, Heidelberg, Germany).

2.12. Histological and immunohistochemical analysis

After the animals were anesthetized, the corneas (up to the limb margin) of rabbits and beagles were dissected under a surgical microscope, with the native cornea and BAC used in paraffin or OCT (4 μm sections) and stained with hematoxylin-eosin (H&E), Masson, and alizarin red (Solarbio, Beijing, China) for observation under a light microscope (BX50, OLYMPUS, China). Immunofluorescence staining was performed using 7 μm frozen sections of NPC and BAC tissues. The primary antibody was *anti*-cytokeratin 3 (ab28260, Abcam, 1:200). The secondary antibody was a goat anti-mouse IgG H&L Alexa Fluor 488 (ab150113, Abcam, 1:500), and the sections were observed under a fluorescence microscope (BX50, OLYMPUS, China).

2.13. Statistical analysis

At least samples were included in the statistical analysis for all experiments, and all data are expressed as the mean ± standard deviation (SD). The statistical trends were analyzed by one-way ANOVA with t tests. A value of $p < 0.05$ was considered to indicate significance, and differences with $p < 0.05$ are indicated with asterisks (*$p < 0.05$, **$p < 0.01$, ***$p < 0.001$, and ****$p < 0.0001$). Statistical analyses were performed using GraphPad Prism 9.0 software.

3. Results

3.1. Biological evaluation of bioartificial cornea

3.1.1. Histological analysis

Bioartificial corneas (BACs) were generated via modification of natural pig corneas (NPCs) after killing bacteria and viruses and removing pyrogens and antigens (Fig. 1A). The whole process was performed in a GMP workshop. The key parts of the process have been verified many times and have good safety and stability. Decellularization of biological tissue is a critical determinant of clinical success [21]. Ionic, nonionic, and zwitterionic detergents solubilize cell membranes and dissociate DNA from proteins, and they are therefore effective in removing cellular material from tissue [22]. Therefore, our decellularization process uses a combination of SDS and CHAPS, which can retain the ECM to the greatest extent but remove cell components to the greatest extent. As shown in Fig. 1B, both the epithelial and stromal layers of the NPC tissue showed abundant cells after cutting with a lamellar knife, and the collagen fibers were arranged in an orderly reticulated structure. The cellular components of the epithelial layer, endocortex and stromal layer in the cornea were effectively removed by the decellularization process, and the decellularized pig cornea (DPC) and BAC tissues retained their fiber network structure after this procedure. Light red collagen staining was observed after HE staining, with no blue-stained nuclear material and no residual cells.

3.1.2. Antigenic analysis

Some studies have proposed a set of minimum criteria to satisfy the description of "decellularized": less than 50 ng of double-stranded DNA (dsDNA) per mg of ECM (dry weight) [23]. Fig. 1D(i) shows that the NPC tissue had a very high DNA content (165.5 ± 14.1 ng/mg), whereas the BAC tissue after decellularization had a very low DNA content (28.5 ± 5.5 ng/mg), with less than 50 ng of DNA per milligram of dry tissue, thus meeting the requirements for DPC tissue. Additionally, α-Gal and Neu5Gc are the main pig-specific xenograft components recognized by human antibodies and are associated with failure of porcine xenografts [24]. The results in Fig. 1D(ii) show that NPCs showed strong expression of the α-Gal epitope (1089.7 ± 138.4 pg/mg). After decellularization, the residual α-Gal in the tissue was largely eliminated. In addition, we also analyzed the removal of another antigenic element (Neu5Gc). The results showed that the decellularization process significantly reduced the content of Neu5Gc in the BACs (Fig. 1D(iii)) without decreasing collagen or glycosaminoglycan (GAG) levels.

3.1.3. Quantitative analysis of extracellular matrix components

As SDS and chaps affect protein−protein interactions, they disrupt the interaction between collagen and proteoglycans, reducing the structural stability of the fiber [25]. To address this limitation [26], we developed a self-crosslinking method that does not require chemical crosslinking agents. Therefore, we quantitatively analyzed the changes in collagen and glycosaminoglycan (GAG) content in the tissues before and after decellularization. For collagen levels (Fig. 1E), the results showed that there was no difference among the three groups before and after decellularization. In addition, compared with that of NPC tissues, the GAG content of DPCs was significantly reduced after decellularization (Fig. 1F). The AHA/CMC-modified cornea (BAC) was modified with hyaluronic acid to compensate for the loss of glycosaminoglycan components induced by the process. Therefore, the decellularization process we designed can maintain ECM collagen and GAG levels to the greatest extent, providing a good tissue structure for improving corneal transparency.

3.2. Composite modification of bioartificial corneas

The detergents, enzymes and physical forces used during decellularization unavoidably alter the corneal extracellular matrix composition and disrupt its ultrastructure [27]. In this work, we modified the surface of DPCs using aldehyde-modified hyaluronic acid (AHA) and carboxymethyl chitosan (CMC) via Schiff's base reaction. The SEM results showed that a layer of endothelial cells was on the surface of the NPCs. The DPCs showed effective removal of cellular components, with only the folds formed by the folding of the collagen fiber structure remaining. BACs modified with AHA/CMC showed a porous hydrogel layer on the surface of the DPCs. The size of the pores ranged from 100 to 300 nm (Fig. 1C). This pore structure is also supported by the observation that the epithelium heals quickly (within 1 week after posterior implantation in animals). We quantitatively analyzed the hyaluronic acid content on the surface of the material. A significantly increased corneal tissue load of 321 ng per milligram was observed compared to that of the control group (Fig. 1I). This also further proves that the hydrogel (AHA/CMC) material was successfully constructed on the surface of the corneal matrix.

3.3. Evaluation of bioartificial corneas

3.3.1. Optical part of bioartificial corneas

To explore the optical properties of the BACs, we tested the light transmittance of the BACs with a high-precision light transmittance meter. As shown in Fig. 1G, the BACs appeared as semitransparent, oval, semiwet films without impurities or defects; they was relatively

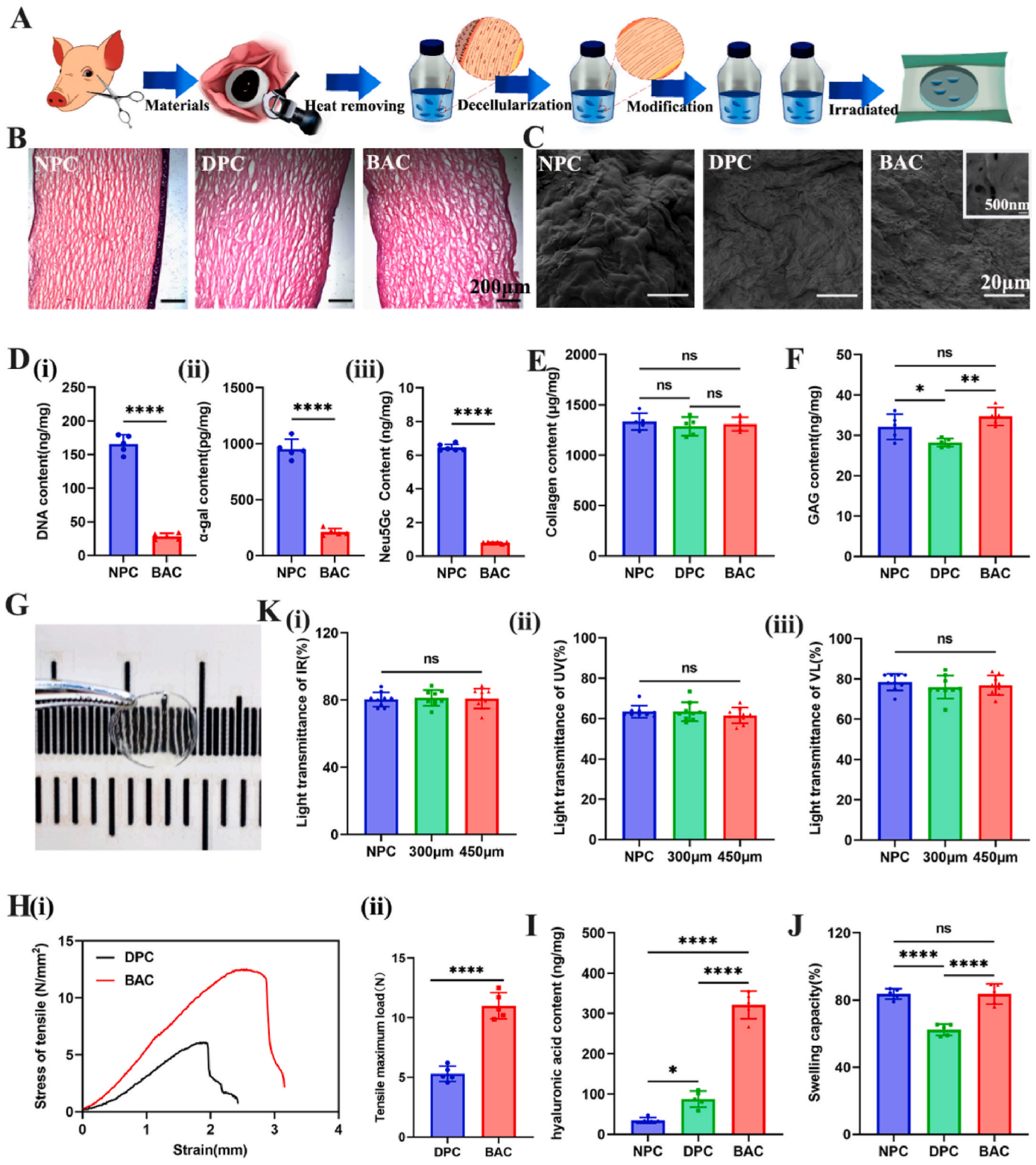

Fig. 1. Safety evaluation of prepared bioartificial corneas. (A) Schematic diagram of the preparation process for bioartificial corneas (BACs). (B) H&E staining after the decellularization process. (C) SEM images of NPCs, DPCs and BACs with porous structures. (D) Quantitative analysis of antigenicity. (i) DNA content analysis, (ii) α-Gal content analysis, (iii) Neu5Gc content analysis. (E) Quantitative analysis of collagen. (F) Quantitative analysis of GAG. (G) Macroscopic appearance of the BAC (thickness: 450 μm). (K) Transmittance analysis of infrared light (i: IR, $\lambda = 940$ nm), ultraviolet light (ii: UV, $\lambda = 365$ nm) and visible light (iii: VL, $\lambda = 380$ nm–760 nm) for the BAC (thickness: 300 μm, 450 μm) and NPC groups. (H) (i) Stress–strain analysis of the BAC and DPC groups. (ii) Tensile maximum load of the BAC and DPC groups. (I) Hyaluronic acid content analysis. (J) Swelling capacity. For statistical analysis, * represents $p < 0.05$, ** represents $p < 0.01$, *** represents $p < 0.001$, and **** represents $p < 0.0001$.

uniform, had good transparency, and exhibited curvature, which allows a better fit after implantation. Then, we analyzed the transmittance of the cornea with an optical transilluminator by testing ultraviolet, infrared and visible light. Corneas freshly excised from porcine eyeballs (NPCs) were used as the main controls. The results in Fig. 1K show that the BACs (thickness = 300 μm or 450 μm) were not significantly different from the NPCs. According to the technical requirements of corneas, the transmittance of IR, UV, and VL should not be less than 80%, 60%, and 75%, respectively. Therefore, our developed BAC meets the national requirements for corneal implant transparency.

3.3.2. Mechanical evaluation of bioartificial cornea

The properties of the corneal stroma determine the mechanical properties of the corneal stromal layer, and the maintenance of tissue tensile strength and suture elasticity can be used as a measure of ECM preservation [28]. Compared with DPCs, BACs can maintain their modified mechanical properties without sacrificing transparency. As shown in the stress–strain curve, at the same shock pressure, BACs have better pressure resistance (Fig. 1Hi). Moreover, the results also show that the maximum tensile strength of BACs is significantly higher than that of DPCs, which further indicates that the BACs have better yield strength and tensile strength (Fig. 1Hii). Therefore, the mechanical properties of BACs modified by self-crosslinking of AHA/CMC were greatly improved. In addition, the BACs retained the ability to withstand 10-0 sutures. The results also showed that the tensile strength of the cornea after suturing was lower than that before suturing, but the BAC group still had a higher value than the control group (Fig. S1).

3.3.3. Swelling rate of the bioartificial corneas

The swelling of the cornea, that is, tissue porosity, was evaluated. Based on the results, DPCs and NPCs showed limited extensibility, which suggested that the elasticity of the tissue structure was compromised to some extent (Fig. 1J). After we modified the hyaluronic acid (AHA/CMC) hydrogel on the surface of DPCs, the porous structure of the hydrogel improved the hydrophilicity of the cornea; the swelling of BACs was not significantly different from that of NPCs, but the hydrophilicity of BACs relieved the symptoms of dry eye after implantation.

3.3.4. Endotoxins, biocompatibility test and virus inactivation

Endotoxin testing was used as a routine quality control test during cornea production. We removed heat sources during BAC production, and the results showed that 30 min of treatment resulted in an endotoxin level of <0.25 EU per cornea (Fig. S2). In addition, in vitro culture of smooth muscle cells was used to evaluate possible acute cytotoxicity associated with the medical materials or their extracts to ensure that the product can meet the cytotoxicity requirements. The results of this experiment were based on a blank control (BC) as a reference (Fig. S3). The cytotoxicity of the positive group (AC) was grade 4 (0–29%), while the cytotoxicity of the control group was grade 0 (RGR ≧ 100%), which indicated that the materials were nontoxic to the cells and met the requirements for registration as an artificial cornea product. To increase the safety of animal-derived medical devices, specific virus inactivation and removal process steps are required during production [29]. The evaluation report includes enveloped viruses, nonenveloped viruses and model viruses from different virus families: porcine parvovirus (PPV), reovirus (Reo 3), vesicular stomatitis virus (VSV) and pseudorabies virus (Vero) [30]. The results showed that the total reduction coefficients of the four indicator viruses reached more than 6 logs (Table S1). Therefore, the validation study demonstrated the effectiveness of the pyrogen treatment process and the electron accelerator irradiation (Co60) treatment process for removing and inactivating virus, indicating that the infectivity of the residual virus in animal-derived materials is greatly reduced and meets the safety standards for animal-derived medical devices.

3.4. Evaluation of bioartificial corneas in vitro

3.4.1. Anti-inflammatory activity

In corneal tissues, natural hyaluronic acid (HA) and carboxymethyl chitosan (CMC) have been shown to induce epithelial cell migration and wound healing [31]. To verify the anti-inflammatory effects of the BACs in vitro, we evaluated LPS-stimulated RAW 264.7 cells. The immunofluorescence results (Fig. 2A) obtained after staining for CD11B to mark monocytes and TNF to mark M_1 inflammatory cells show a comparison of the LPS group and control group. The DPC group and BAC group showed very weak TNF-α fluorescence; in contrast, the BACs exhibited a high CD11B fluorescence intensity in monocyte cells. Therefore, the results proved that the BACs inhibited inflammation in the graft to some degree.

We also validated the anti-inflammatory capacity of the cornea by quantitatively analyzing the release of NO and inflammatory factors. BACs significantly affected NO release in LPS-treated cells. NO release was significantly reduced in the BAC group (8.56%) compared to the LPS group (Fig. 2B). The rate of inhibition of NO release for BAC was 91.44%. These results further verify the above conclusion. The expression of the inflammatory factor IL-1β was significantly lower in the BAC group than in the other three groups (Fig. 2D). This indicates that BAC can inhibit the production of proinflammatory cytokines and exhibit anti-inflammatory activity. In addition to proinflammatory factors such as interleukins, TNF-α and TNF-β play important roles in local and cyclic inflammatory responses [34]. BAC also greatly reduced the expression of TNF-α (Fig. 2C). Therefore, HA and CMC released by BACs through surface-modified hydrogels can significantly downregulate the proinflammatory factors TNF-α and IL-1β to enhance the alleviation of corneal inflammation and other complications in vivo.

3.4.2. Antibacterial activity evaluation

To analyze the antibacterial activity of BACs, the plate count method was used with two representative bacteria (*E. coli* and *S. aureus*). First, the release of HA from BACs was assessed, and it was found that HA was released rapidly in the first 24 h (Fig. S3C). Therefore, we verified the antibacterial activity of BACs by the plate counting method. The results showed that unlike the DPCs, the BACs had antibacterial properties (Fig. 2E). Within 24 h of contact with bacteria, they could effectively inhibit the growth of bacteria. However, after 48 h of contact culture, the number of drug-resistant bacteria increased rapidly, and the bacteria could grow through the cornea (Fig. S4). Therefore, BACs have a mild antibacterial effect, with an antibacterial duration of approximately 24 h.

3.5. Evaluation of bioartificial corneas in rabbits

3.5.1. Transparency assessment

BAC grafts (thickness = 300 μm) were implanted into rabbit eyes by lamellar keratoplasty [32]. The slit lamp results showed that the corneal graft was implanted into the eyeball and fit well; there was no ulceration at the suture, and the graft had some degree of transparency. Within 3–7 days postsurgery, the corneal grafts were well preserved, without large areas of ulceration, edema, or obvious inflammation (Fig. S5). From 1 month postsurgery, the suture gradually faded, and the graft became transparent (Fig. 3A). At 3 months postsurgery, the suture and corneal scar were almost invisible, and the graft was more transparent. From 6 months to 12 months postsurgery, eyes implanted with the grafts were similar to normal eyeballs. Fluorescein staining of BACs further verified the transparent nature of the BAC after half-layer keratoplasty (Fig. 3B). At 3–7 days postsurgery, the corneal scar area (green scale) was clearly visible. The scar area decreased, and the residual graft was in the middle. At 2 weeks postsurgery, the suture was desalinated, and the scar area remained small; the corneal suture disappeared without corneal scarring within 1 month.

OCT images of the central 5 mm area and the corresponding operated

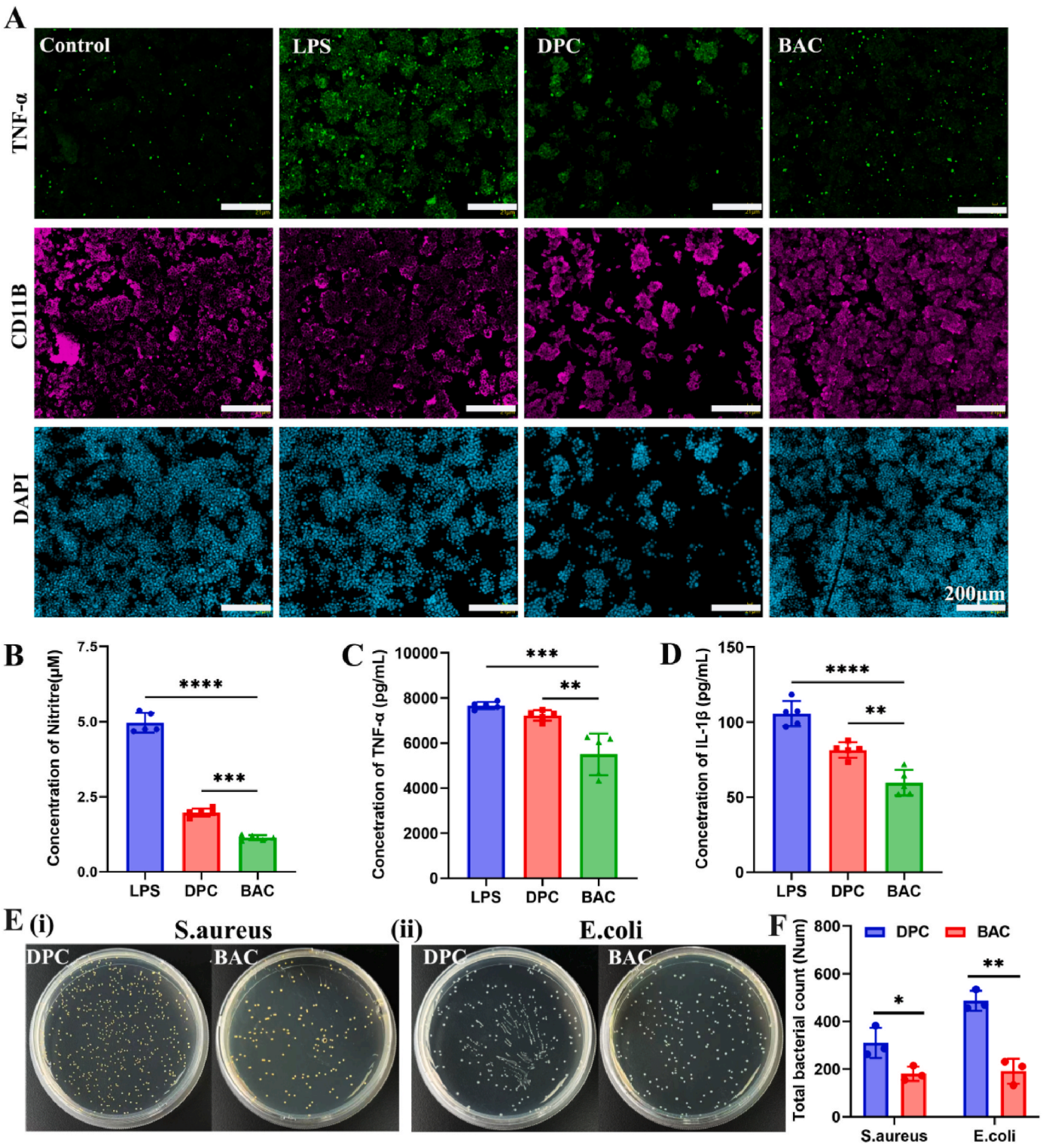

Fig. 2. Anti-inflammatory and antibacterial evaluation of BACs. (A) Immunofluorescence staining images of LPS-stimulated RAW 264.7 cells in the presence of DPCs and BACs. (B) Levels of nitrites. (C) Expression of the inflammatory factor TNF-α. (D) Expression of the inflammatory factor IL-1β. (E) Antibacterial effect of BACs and DPCs on *S. aureus* (i) and *E. coli* (ii). (F) Total bacterial count for *S. aureus* and *E. coli*.

eyes indicated that the thickness of the corneal implant area gradually stabilized over time and that the transparency gradually approached that of the normal eye (Fig. S5). The results further verified that BACs can rapidly become transparent. We further measured the thickness changes of the BAC graft after transplantation. The graft had a central thickness of 417 μm one month after surgery, 391 μm 6 months after surgery, and 394 μm 12 months after surgery. The corneal thickness slightly decreased in the first three months and later stabilized.

3.5.2. *Evaluation of epithelization and nerve regeneration*

We further verified that BACs can quickly achieve in vivo epithelization and nerve regeneration. The results of IVCM showed that many

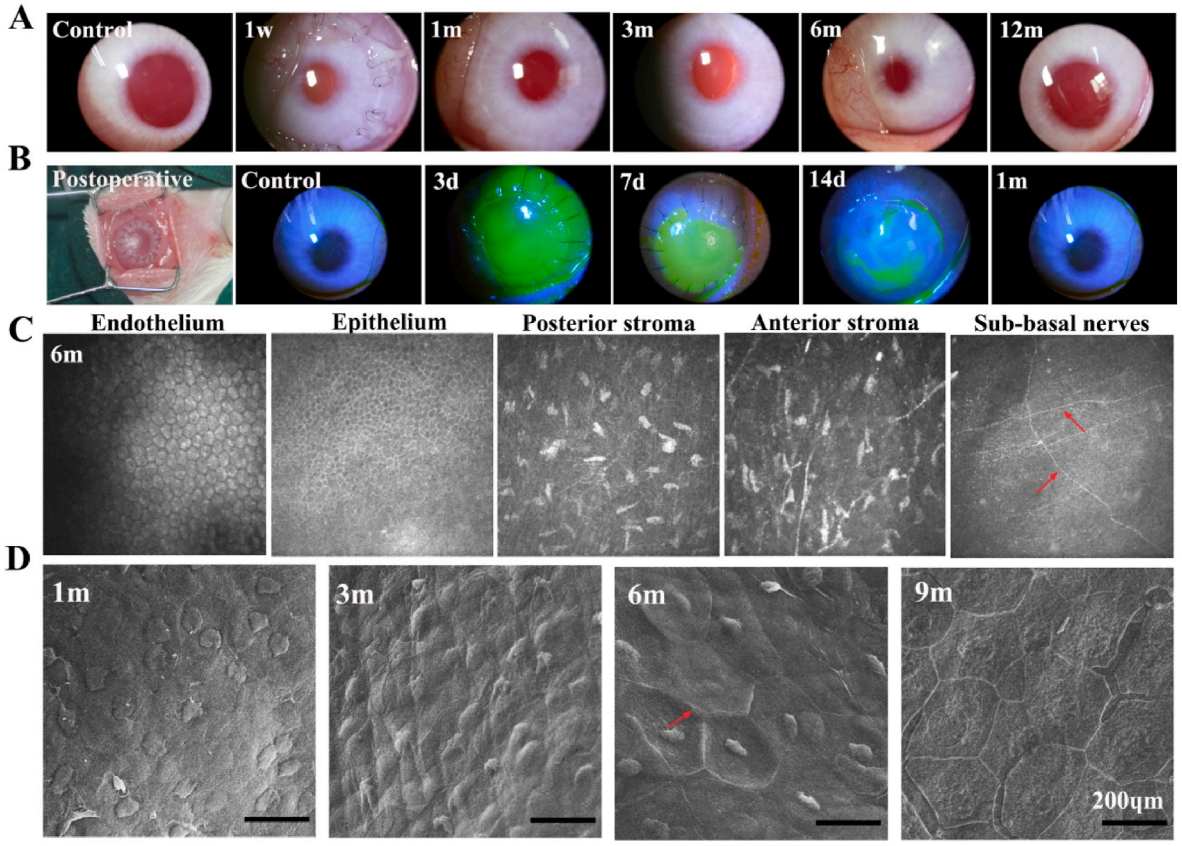

Fig. 3. Evaluation of bioartificial corneas in rabbits. (A) Local views of the slit lamp results at different time points. (B) Postoperative image and fluorescein staining. Green scale: corneal scar area. (C) In vivo confocal microscopy (IVCM) at 6 months postsurgery. Red arrow: nerve fibers. (D) SEM of epithelial cells in vitro. Red arrow: endothelial border.

uniformly distributed endothelial cells were observed after 1–3 months, but the intercellular space was large. The epithelium-covered area reached 90%, with only a small defect area. The stromal layer began to become loose but contained many stromal cells, with a small amount of angiogenesis and optic nerve plexus ingrowth. After 6 months (Fig. 3C), the epithelium and endodermis adopted a stable morphology and grew well. In particular, epithelial cells in the implant bed had an orderly arrangement and close interactions between cells. Signs of neurite growth under the basement could be seen after 1 month, and sparse nerve fibers were found in the grafts around the eyes (Fig. S5). The morphology of these regenerated nerve fibers was similar to the normal morphology of nerve fibers in the cornea after 6 months and were longer

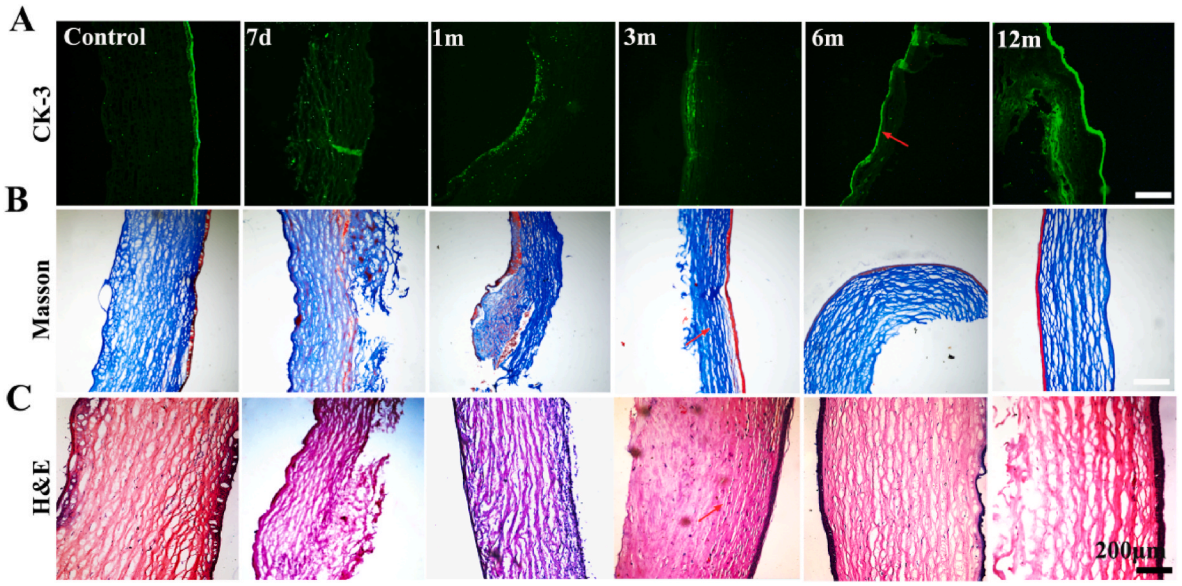

Fig. 4. Histological evaluation of bioartificial corneas in rabbits. (A) Corneal epithelial layers (CK-3); red arrow: corneal epithelial differentiation. (B) Stromal layers (Masson); red arrow: collagen fibers. (Ci) Recellularization (H&E) evaluation; red arrow: collagen fibers between the corneal graft and tissue.

and more regular. We also analyzed endothelial cells by scanning electron microscopy. Fig. 3D shows that the morphology of corneal cells tended to be normal at 1 month and 3 months, but the boundaries were not clear. At 6 months, the nuclei of corneal cells were obviously visible, the edges were hexagonal, and the boundaries were clear. In addition, the epithelial layer was intact and similar to that of normal eyes at 9 months, which was consistent with previous results.

3.5.3. Histological evaluation

Corneal tissue was removed at different time points to analyze graft degradation, cell migration and regeneration, and changes in calcification. Immunofluorescence staining was used to assess the CK-3 phenotype of the recellularized epithelium. The results showed that the epithelial layer of the control group had a strong CK-3 signal (Fig. 4A). Early epithelial cells implanted with BACs began to heal, but the epithelial cells had not yet grown. After 3 months, the signal of epithelial cells gradually increased, and the corneal epithelial cells grew well. Through Masson staining and H&E staining, we further analyzed the changes in collagen structure and the changes in each layer of cells, and implants were divided into three growth stages in vivo (Fig. 4B–C). In the early stage (one month), the epithelial layer gradually began to form, and the loose stroma layer also began to adopt an orderly arrangement. The cells gradually migrated from the implantation bed to the corneal scaffold, but the number of cells was small. The second stage is the rapid growth process (6 months). The epithelial layer has been fully formed, most of the stromal cells are scattered in the corneal stent, and the collagen structure in the stent is close to that of normal tissue. The final stage is the stable stage of corneal tissue. From 6 months to 12 months, the implantation bed was completely consistent, and there was no obvious dividing line between the implant and the normal tissue.

The previous results show that BAC has good biocompatibility in vivo, but as a long-term graft in vivo, we still need to verify whether it becomes calcified in vivo. The results of long-term alizarin red staining (Fig. S5) showed that the corneal endothelial cells in the cross section

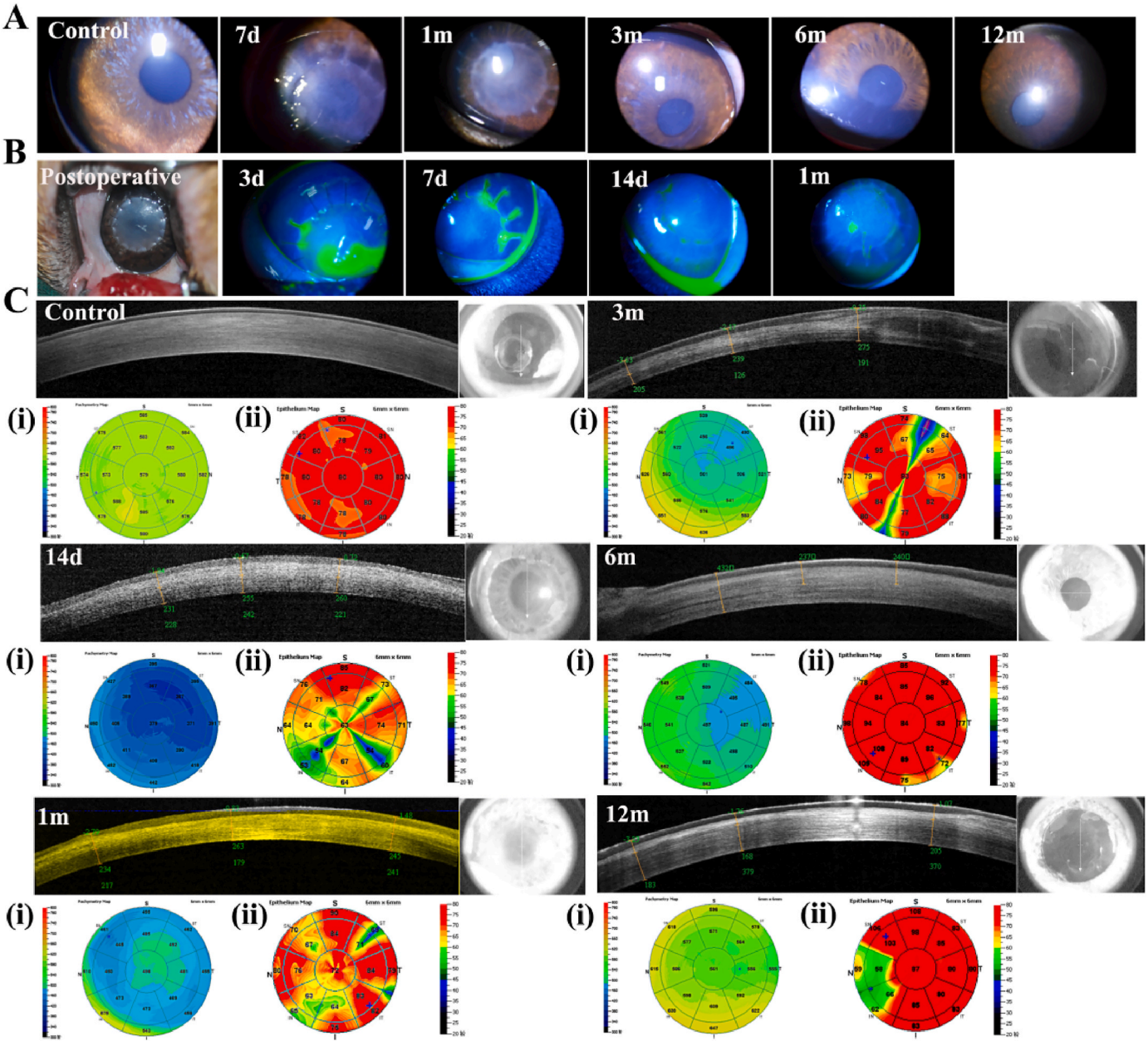

Fig. 5. In vivo evaluation of bioartificial corneas in beagles. (A) Local views of the slit lamp at different time points. (B) Postsurgery and corneal fluorescein staining, green scale: corneal scar area. (C) Optical coherence tomography (OCT) images. (i) Pachymetry map and (ii) Epithelium map.

had clear hexagonal boundaries, were orange–red, were consistent in depth and were arranged in a mosaic pattern. The stromal layer in the longitudinal section was arranged in a grid-like order, and no calcification was noted in the staining results, which also indicated that the cornea did not cause adverse reactions in vivo.

3.6. Large animal evaluation of bioartificial corneas

3.6.1. Transparency assessment

To ensure the preclinical effectiveness of the BACs, we also evaluated 30 beagles after lamellar keratoplasty [33]. This study was designed to use the left eye, with a 450 μm thickness for the BAC. Slit lamp analysis of the implanted graft at different times of corneal scar healing and monitoring of transparency changes were performed. Compared with the results obtained in rabbits, corneal epithelial healing and rapid transparency in beagles were more ideal. After 3 months, the graft was completely transparent, with no suture marks, and the corneal clarity gradually approached that of normal eyes (Fig. 5A). Corneal epithelial healing was analyzed by fluorescein staining throughout the area of the corneal scar (green scale). Seven days after the operation, the epithelial layer of the graft was completely healed, and only the suture was defective in the epithelium (Fig. 5B). After 14 days to 1 month, the epithelium gradually healed and became transparent.

We further analyzed the overall morphology of the cornea after implantation and healing of the graft and substrate by using OCT (Fig. 5C). The OCT results of the control group showed that the central area thickness was 579 μm and 80 μm. Within contrast to the control group, the graft gradually attached to the substrate at 14 days post-surgery, but the thickness of the graft was thicker, and epithelial healing was not optimal. At 1–3 months, the graft had become completely transparent, with low reflectivity and persistent thinning of the cornea. After 6 months, the implant and substrate were clear, and the transparency was similar to that of normal eyes. We further verified the above analysis results from the changes in corneal thickness (Fig. 5i) and epithelial thickness (Fig. 5(ii)). After 6–12 months, the corneal thickness became uniform in the 5 mm area without swelling, and the epithelial thickness reached the epithelial thickness of normal eyes.

3.6.2. Recellularization evaluation

In this work, we also evaluated the tissue regeneration of BACs in

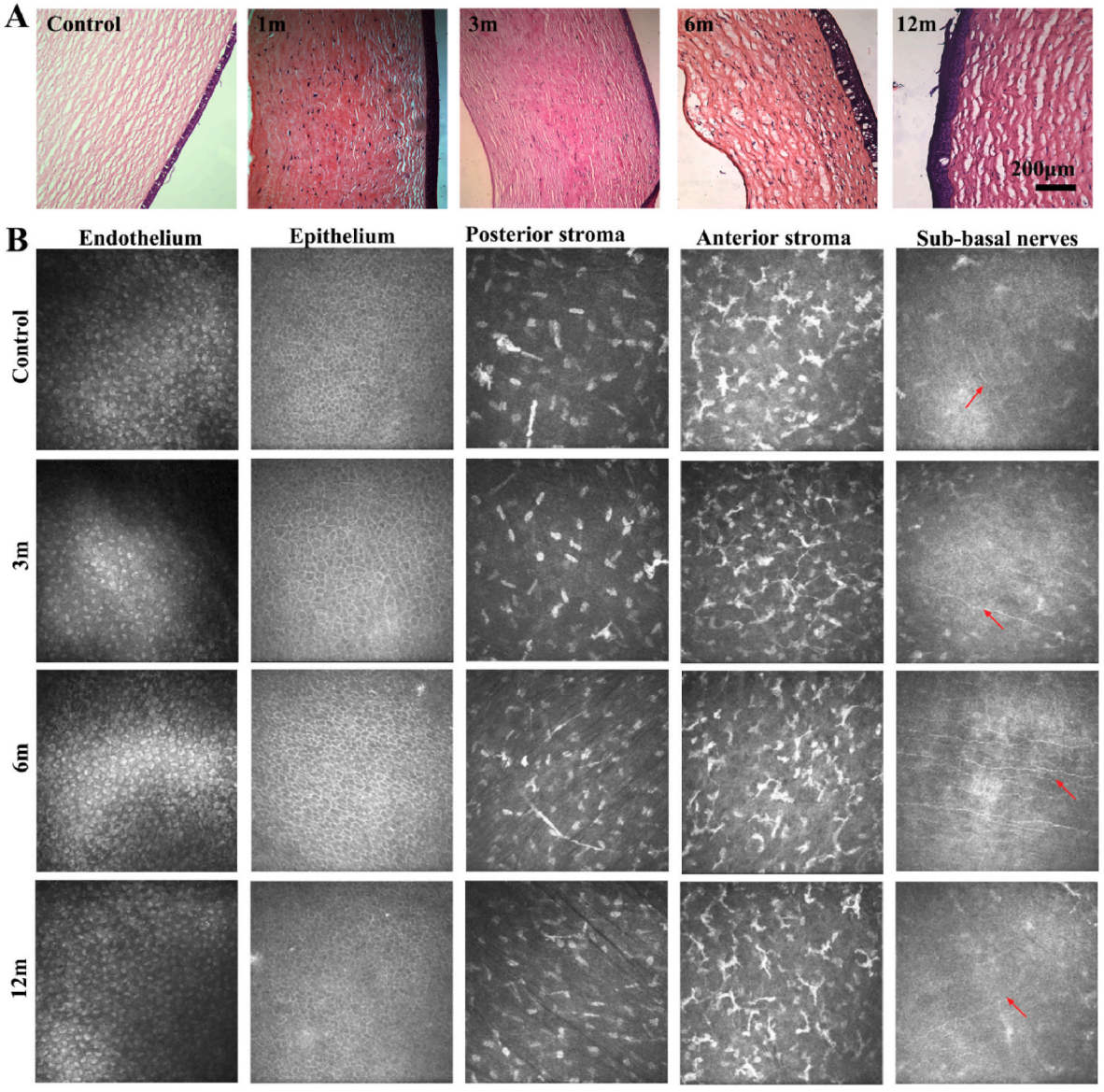

Fig. 6. Recellularization evaluation of bioartificial corneas in beagles. (A) Histological evaluation (H&E staining). (B) In vivo confocal microscopy examination, red arrow: nerve fibers.

large animals. Cell regeneration, epithelialization, calcification, and tissue structural changes were analyzed. H&E staining (Fig. 6A) showed that the stromal layer gradually entered the stromal cells with time, and the endothelial cell layer was thickened. Immunostaining of CK-3 (Fig. S6) showed that a weak epithelial CK-3 signal was visible 1 month after surgery, but the signal intensified after 3 months. Masson staining and Alizarin Red staining showed that the collagen fiber structure was close to that of normal tissue after 3 months. From the perspective of histology, the time required for cell regeneration and the change in scaffold lamellar structure is much shorter than the treatment time in rabbits, which is also consistent with the previous results for in vivo transparency and epithelialization. Therefore, we believe that the results in beagles are more ideal than those in rabbits, and the efficacy is more obvious.

Compared with the growth of the endodermis, epithelium, stroma and nerve plexus in normal eyes, the BAC showed a complete hexagonal shape 3 months after epithelial cell chimerism. The intercellular space increasingly decreased, and the basement had a faintly visible nerve plexus distribution. In addition, the distribution of stromal cells in the stroma layer before and after revealed an orderly arrangement, and the corneal nerve line was clearly visible. Thus, we can see from the in vivo analysis of large animals that the in vivo effect is good, and the degree of corneal transparency and recellularization is good.

3.6.3. Evaluation of primates monkeys in vivo

To verify the preclinical efficacy of the corneas, we used five monkeys to analyze the transparency and epithelialization of BACs after implantation [34]. Unlike in rabbits and beagles, fluorescein staining showed that the epithelial layer healed rapidly within 7 days (Fig. 7A). Additionally, the grafts were opaque and swollen at 14 days. After 37 days, the transparency of the grafts was good, and the corneal scar gradually disappeared. Finally, at 79 days, the monkeys had normal vision (Fig. 7B). Therefore, BACs are more biocompatible and can become transparent more quickly in monkeys.

3.7. Efficacy evaluation of bioartificial corneas in rabbits and beagles

In this work, a self-cross-linking corneal stromal substitute (BAC) that does not require a cross-linking agent was developed. The previous animal test results showed that the BAC quickly became transparent and underwent epithelial healing after corneal implantation (Fig. 8A). We mainly chose deep lamellar transplantation for corneal transplantation. Rabbits, beagles and primates were used as experimental animals. We performed statistical analysis of the data from both rabbits and beagles. Here, we assessed the degree of corneal opacity in 25 rabbits and 35 beagles at 1 month, 2 months, 3 months and 6 months after BAC transplantation and whether we could see the iris texture and pupil. The results showed that 5 out of 10 rabbits had grade 1 or 0 graft transparency within 30 days after BAC transplantation. Within 60 days, the transparency of the implant reached grade 1 or 0 in 2 rabbits (Fig. 8B). At 180 days, the transparency of all rabbit implants reached grade 1 or 0. As shown in Fig. 8C, after short-term observation, 7 beagles reached grade 1, and 10 beagles reached grade 1 or 0 after 90 days (completely transparent, with no ulcer or turbidity). The iris texture and pupil were obviously visible.

Complete corneal reepithelialization plays an important role in the survival of BAC grafts [35]. This epithelialization can improve the structure of the BCA graft, cover the wound edge to heal the wound, and provide a robust barrier function for the entire ocular surface. As shown in Fig. 8C, regarding the epithelial healing area at 3 and 7 days after implantation, the beagles healed better than the rabbits, and the graft surface epithelialization rate was more than 50%. After 14 days, all rabbit sutures were loose, except for a few small focal spots, and most of the graft was re-epithelialized. In beagles, the corneal re-epithelial healing degree reached more than 70% in 14 days and after 1 month. Re-epithelialization was complete in all animals. No clinical signs of

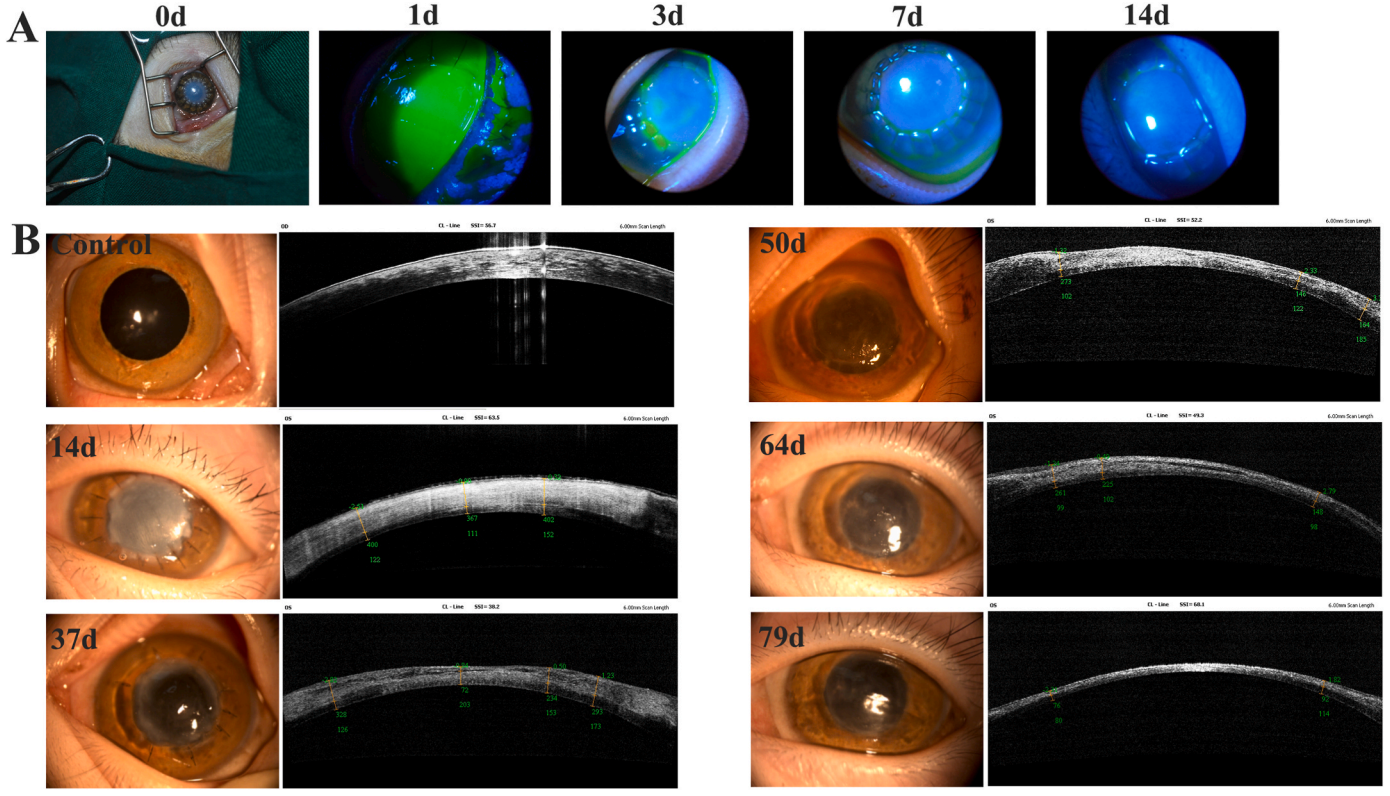

Fig. 7. In vivo evaluation of bioartificial corneas in primates monkeys. (A) Postsurgery and corneal fluorescein staining, green scale: corneal scar area. (B) Local views of the slit lamp and optical coherence tomography (OCT) images at different time points.

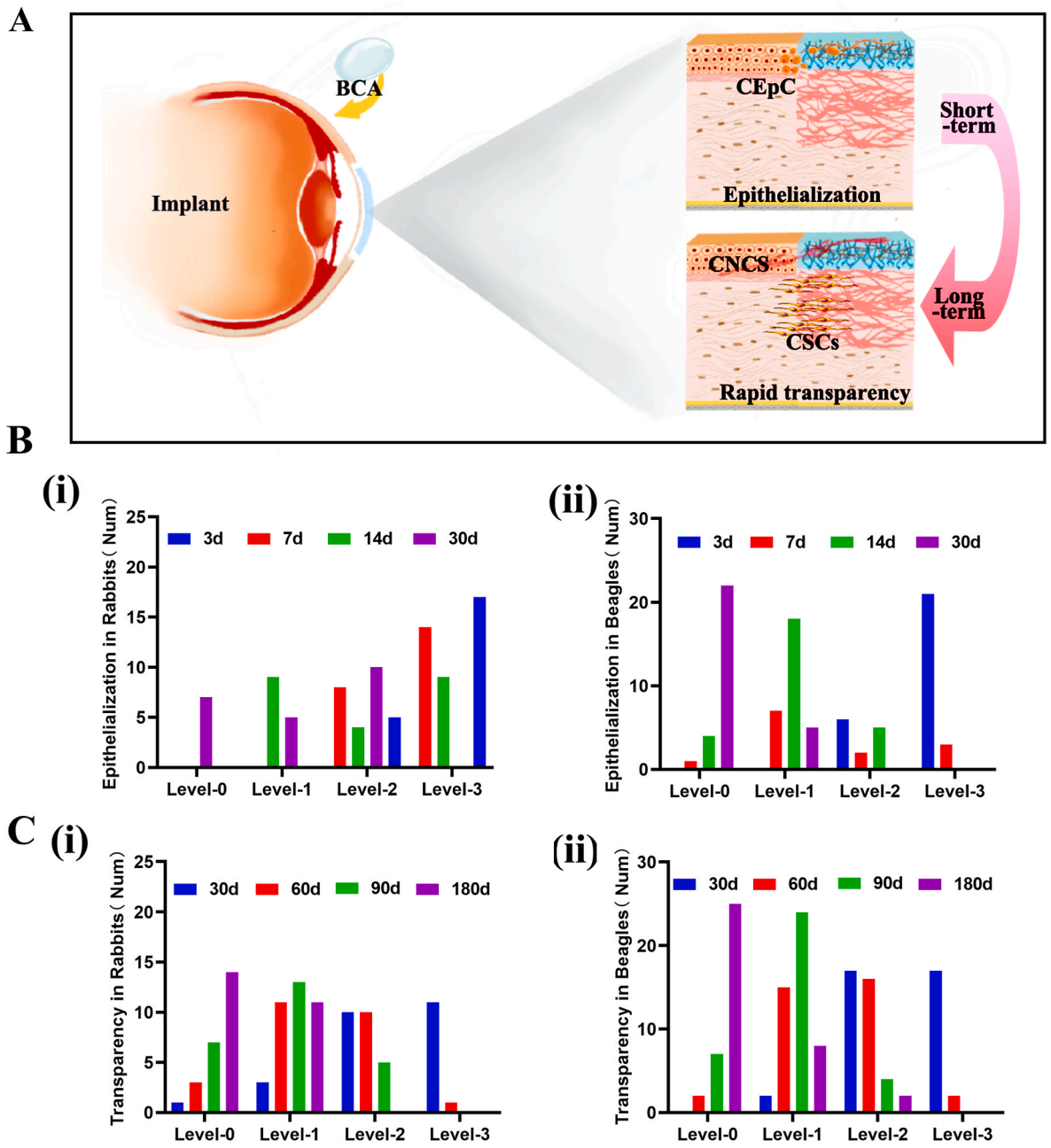

Fig. 8. Evaluation of transparency and epithelial healing after transplantation. (A) Schematic diagram of the surface modification process of BACs and rapid cellularization and hyalinization in vivo after lamellar keratoplasty. (B) Transparency in rabbits (Num = 25). (C) Transparency in beagles (Num = 35). (D) Epithelial healing in rabbits (Num = 22). (E) Epithelial healing in beagles (Num = 27).

graft rejection (pain, light sensitivity) or neovascularization were found throughout the study period.

4. Discussion

The DPC stroma may be a promising source of material to overcome the limited availability of human donors [35]. Unfortunately, collagen and elastin in the ECM are exposed to enzymatic biodegradation in the host [36]. According to the requirements for medical device research and development, our BAC passed the registration test of the State Food and Drug Administration (No: QZ201701672), and the cornea was tested physically, chemically, mechanically, and for harmful substances and microorganisms. The results show that the BACs have good transparency, mechanical strength and biocompatibility, which is consistent with the requirements of major medical devices. In addition, the entire preparation process can substantially reduce immunogenicity, effectively inactivate viruses, remove heat sources, and ensure the safe and effective use of animal-derived products.

The role of corneal cells in the corneal stromal remodeling process is crucial [37]. On the one hand, compared with other transplants, BAC grafts produce more significant cellular infiltration after implantation of the graft. We found that after one month, gradual stromal cell remodeling was completed; after 2 months, inflammation subsided, and the corneal tissue morphology was stable; and at 1 year, the corneal integrity was good. On the other hand, BAC successfully stimulated endogenous cells, and endogenous nerves also grew into the graft. The nerve growth of 39 animals at different stages after BAC implantation was analyzed by in vivo confocal microscopy. The results showed that the tissue structure was very close to that of the normal cornea at 8 months after transplantation. In addition, Masson staining indicated that the

tissue structure of the BAC transplants was very similar to that of the normal cornea (Masson). Alizarin red staining can reflect tissue calcification. BAC grafts were implanted into rabbits and had no calcification after one year, which is very similar to the normal cornea (ARS). Therefore, the corneal lamellar structure remained good after the BAC was transplanted to the ocular surface in rabbits and beagles. Epithelialization was essentially completed within 2 weeks, and the epithelial basement membrane appeared within one month. These results showed that the epithelial and stromal layers had good regenerative repair function after BAC implantation.

The results obtained for our BAC indicate that it is safe to produce as a class III medical device, and has the effects of rapid epithelialization and transparency as well as tissue regeneration in various animals. Hence, the number of cases treated in clinical practice is higher for this medical device than for other corneal stroma products.

5. Conclusion

Although previous clinical studies have focused on human donor tissues, bioengineered implant tissues are essential for reducing the global burden of corneal blindness. Although most clinical studies have made significant progress with acellular tissues [34], the application scope is very limited [33]. For example, 'AiNear' is the world's first and only bioengineered corneal product available on the market [38,39]. It may be suitable for a small number of people with corneal blindness and therefore cannot fundamentally resolve the donor cornea shortage [40]. In addition, to obtain good mechanical properties, the optimal crosslinking method was studied to prevent the destruction of collagen by excessive crosslinking. From a safety perspective, we have developed a commercially and clinically feasible GMP-grade cornea, based on natural noncellular bioderived materials from animal sources, with killing of bacteria and viruses, removal of pyrogens and antigens, and composite modification. It has mechanical strength and elasticity close to those of the normal human cornea, and clear antibacterial and anti-inflammatory properties in vitro.

From the perspective of efficacy, previously studied corneal products did not achieve sufficient corneal transparency in vivo or have sufficient corneal cell-filled scaffolds. The BAC we developed was evaluated in preclinical animals. After implantation, the turbidity period was short. The suture repair moved quickly, and there was no scar visible to the naked eye. Corneal epithelial cells can grow rapidly into the graft covering and form a smooth epithelial layer. Stromal cells can adhere, grow and differentiate in the collagen layer, resulting in extracellular matrix production. The product gradually fuses with autologous corneal tissue after transplantation to repair the damaged cornea, eventually acquiring a structure and function similar to those of the normal cornea and restoring vision while beautifying the eyeball. Most importantly, this product can be used as a corneal equivalent substitute for in vitro reconstruction to solve the problem of donor corneal insufficiency, making it an ideal graft for corneal transplantation in patients with severe corneal injury.

Ethics approval and consent to participate

This study was designed to examine the safety and effectiveness evaluation of bioartificial cornea in preclinical research. The rabbit, beagle and Primate monkey models were used to determine the in vivo biocompatibility. All animal experiments were approved by the Ethics Committee of the Army Medical University, China. Experiments were carried out in accordance with the regulations of ethical approval for research on laboratory animals.

CRediT authorship contribution statement

Yansha Hao: Formal analysis, Methodology, Writing-original draft, Writing-review & editing. **Jingting Zhou:** Formal analysis, Methodology, Writing-original draft. **Ju Tan:** Formal analysis, Methodology, Writing-original draft. **Feng Xiang:** Methodology, Formal analysis. **Mingcan Yang:** Methodology, Formal analysis. **Gang Li:** Methodology, Formal analysis. **Zhongliang Qin:** Methodology, Formal analysis. **Jun Yao:** Funding acquisition, Project administration. **Lingqin Zeng:** Writing-original draft, Methodology. **Wen Zeng:** Funding acquisition, Methodology, Investigation. **Chuhong Zhu:** Funding acquisition, Conceptualization, Supervision, Writing - review & editing.

Declaration of competing interest

The authors declare that they have no known competing financial interests or personal relationships that could have appeared to influence the work reported in this paper.

Acknowledgements

This work was supported by National Science Fund for Distinguished Young Scholars (No. 31625011), the National Key Research and Development Program (No.2016YFC1101100).

Appendix A. Supplementary data

Supplementary data to this article can be found online at https://doi.org/10.1016/j.bioactmat.2023.07.005.

References

[1] S.C. Tidke, P. Tidake, A review of corneal blindness: causes and management, Cureus 14 (10) (2022), e30097, https://doi.org/10.7759/cureus.30097.
[2] J.P. Whitcher, M. Srinivasan, M.P. Upadhyay, Corneal blindness: a global perspective, Bull. World Health Organ. 79 (3) (2001) 214–221. https://pubmed.ncbi.nlm.nih.gov/11285665/.
[3] V. Lamm, H. Hara, A. Mammen, D. Dhaliwal, D.K. Cooper, Corneal blindness and xenotransplantation, Xenotransplantation 21 (2) (2014) 99–114, https://doi.org/10.1111/xen.12082.
[4] R.N. Palchesko, S.D. Carrasquilla, A.W. Feinberg, Natural biomaterials for corneal tissue engineering, repair, and regeneration, Advanced healthcare materials 7 (16) (2018), e1701434, https://doi.org/10.1002/adhm.201701434.
[5] K. Nishida, Tissue engineering of the cornea, Cornea 22 (7 Suppl) (2003) S28–S34, https://doi.org/10.1097/00003226-200310001-00005.
[6] C.E. Ghezzi, J. Rnjak-Kovacina, D.L. Kaplan, Corneal tissue engineering: recent advances and future perspectives, Tissue engineering, Part B, Reviews 21 (3) (2015) 278–287, https://doi.org/10.1089/ten.TEB.2014.0397.
[7] M. Ahearne, J. Fernández-Pérez, S. Masterton, P. Madden, P.B.J.A.F. Materials, Designing Scaffolds for Corneal Regeneration, 2020, p. 30, https://doi.org/10.1002/adfm.201908996, undefined.
[8] Y. Zeng, J. Yang, K. Huang, Z. Lee, X. Lee, A comparison of biomechanical properties between human and porcine cornea, J. Biomech. 34 (4) (2001) 533–537, https://doi.org/10.1016/s0021-9290(00)00219-0.
[9] A. Isidan, S. Liu, P. Li, M. Lashmet, L.J. Smith, H. Hara, D.K.C. Cooper, B. Ekser, Decellularization methods for developing porcine corneal xenografts and future perspectives, Xenotransplantation 26 (6) (2019), e12564, https://doi.org/10.1111/xen.12564.
[10] A. Gilpin, Y. Yang, Decellularization strategies for regenerative medicine: from processing techniques to applications, BioMed Res. Int. 2017 (2017), 9831534, https://doi.org/10.1155/2017/9831534.
[11] M. Dong, L. Zhao, F. Wang, X. Hu, H. Li, T. Liu, Q. Zhou, W. Shi, Rapid porcine corneal decellularization through the use of sodium N-lauroyl glutamate and supernuclease, J. Tissue Eng. 10 (2019), 2041731419875876, https://doi.org/10.1177/2041731419875876.
[12] R. Sharifi, Y. Yang, Y. Adibnia, C.H. Dohlman, J. Chodosh, M. Gonzalez-Andrades, Finding an optimal corneal xenograft using comparative analysis of corneal matrix proteins across species, Sci. Rep. 9 (1) (2019) 1876, https://doi.org/10.1038/s41598-018-38342-4.
[13] H. Hara, D.K. Cooper, The immunology of corneal xenotransplantation: a review of the literature, Xenotransplantation 17 (5) (2010) 338–349, https://doi.org/10.1111/j.1399-3089.2010.00608.x.
[14] J.S. Lee, S.U. Lee, C.Y. Che, J.E. Lee, Comparison of cytotoxicity and wound healing effect of carboxymethylcellulose and hyaluronic acid on human corneal epithelial cells, Int. J. Ophthalmol. 8 (2) (2015) 215–221, https://doi.org/10.3980/j.issn.2222-3959.2015.02.01.
[15] S.S. Mahdavi, M.J. Abdekhodaie, S. Mashayekhan, A. Baradaran-Rafii, A. R. Djalilian, Bioengineering approaches for corneal regenerative medicine, Tissue engineering and regenerative medicine 17 (5) (2020) 567–593, https://doi.org/10.1007/s13770-020-00262-8.

[16] W. Xu, Z. Wang, Y. Liu, L. Wang, Z. Jiang, T. Li, W. Zhang, Y. Liang, Carboxymethyl chitosan/gelatin/hyaluronic acid blended-membranes as epithelia transplanting scaffold for corneal wound healing, Carbohydr. Polym. 192 (2018) 240–250, https://doi.org/10.1016/j.carbpol.2018.03.033.
[17] G. Janarthanan, H.S. Shin, I.G. Kim, P. Ji, E.J. Chung, C. Lee, I. Noh, Self-crosslinking hyaluronic acid-carboxymethylcellulose hydrogel enhances multilayered 3D-printed construct shape integrity and mechanical stability for soft tissue engineering, Biofabrication 12 (4) (2020), 045026, https://doi.org/10.1088/1758-5090/aba2f7.
[18] W.H. Chang, P.Y. Liu, M.H. Lin, C.J. Lu, H.Y. Chou, C.Y. Nian, Y.T. Jiang, Y.H. Hsu, Applications of hyaluronic acid in ophthalmology and contact lenses, Molecules 26 (9) (2021), https://doi.org/10.3390/molecules26092485.
[19] Y. Liu, L. Ren, Y. Wang, Crosslinked collagen-gelatin-hyaluronic acid biomimetic film for cornea tissue engineering applications, Materials science & engineering, C, Materials for biological applications 33 (1) (2013) 196–201, https://doi.org/10.1016/j.msec.2012.08.030.
[20] M.N. Collins, C. Birkinshaw, Hyaluronic acid based scaffolds for tissue engineering–a review, Carbohydr. Polym. 92 (2) (2013) 1262–1279, https://doi.org/10.1016/j.carbpol.2012.10.028.
[21] T.W. Gilbert, T.L. Sellaro, S.F. Badylak, Decellularization of tissues and organs, Biomaterials 27 (19) (2006) 3675–3683, https://doi.org/10.1016/j.biomaterials.2006.02.014.
[22] A.P. Lynch, M. Ahearne, Strategies for developing decellularized corneal scaffolds, Exp. Eye Res. 108 (2013) 42–47, https://doi.org/10.1016/j.exer.2012.12.012.
[23] P.M. Crapo, T.W. Gilbert, S.F. Badylak, An overview of tissue and whole organ decellularization processes, Biomaterials 32 (12) (2011) 3233–3243, https://doi.org/10.1016/j.biomaterials.2011.01.057.
[24] S.M. Li, F.L. Bai, W.J. Xu, Y.B. Yang, Y. An, T.H. Li, Y.H. Yu, D.S. Li, W.F. Wang, Removing residual DNA from Vero-cell culture-derived human rabies vaccine by using nuclease, Biologicals : J. Int. Assoc. Buddhist Stud. 42 (5) (2014) 271–276, https://doi.org/10.1016/j.biologicals.2014.06.005.
[25] J. Fernández-Pérez, M. Ahearne, The impact of decellularization methods on extracellular matrix derived hydrogels, Sci. Rep. 9 (1) (2019), 14933, https://doi.org/10.1038/s41598-019-49575-2.
[26] H. Yang, Q. Tan, H. Zhao, Progress in various crosslinking modification for acellular matrix, Chin. Med. J. 127 (17) (2014) 3156–3164.
[27] Y. Shao, Y. Yu, C.G. Pei, Y. Qu, G.P. Gao, J.L. Yang, Q. Zhou, L. Yang, Q.P. Liu, The expression and distribution of α-Gal gene in various species ocular surface tissue, Int. J. Ophthalmol. 5 (5) (2012) 543–548, https://doi.org/10.3980/j.issn.2222-3959.2012.05.01.
[28] N. Formisano, C. van der Putten, R. Grant, G. Sahin, R.K. Truckenmüller, C.V. C. Bouten, N.A. Kurniawan, S. Giselbrecht, Mechanical properties of bioengineered corneal stroma, Advanced healthcare materials 10 (20) (2021), e2100972, https://doi.org/10.1002/adhm.202100972.
[29] S.Y. Yu, F.Y. Li, H.M. Wang, Regenerative implantable medical devices: an overview, Health Inf. Libr. J. 33 (2) (2016) 92–99, https://doi.org/10.1111/hir.12146.
[30] J. Hodde, M. Hiles, Virus safety of a porcine-derived medical device: evaluation of a viral inactivation method, Biotechnol. Bioeng. 79 (2) (2002) 211–216, https://doi.org/10.1002/bit.10281.
[31] L.F. Baeva, D.B. Lyle, M. Rios, J.J. Langone, M.M. Lightfoote, Different molecular weight hyaluronic acid effects on human macrophage interleukin 1β production, J. Biomed. Mater. Res. 102 (2) (2014) 305–314, https://doi.org/10.1002/jbm.a.34704.
[32] X.C. Lin, Y.N. Hui, Y.S. Wang, H. Meng, Y.J. Zhang, Y. Jin, Lamellar keratoplasty with a graft of lyophilized acellular porcine corneal stroma in the rabbit, Vet. Ophthalmol. 11 (2) (2008) 61–66, https://doi.org/10.1111/j.1463-5224.2008.00601.x.
[33] A. Lavaud, M.E. Kowalska, K. Voelter, S.A. Pot, A. Rampazzo, Penetrating keratoplasty in dogs using acellular porcine corneal stroma (BioCorneaVet™): a prospective pilot study of five cases, Vet. Ophthalmol. 24 (5) (2021) 543–553, https://doi.org/10.1111/vop.12884.
[34] S. Li, M. Li, L. Gu, L. Peng, Y. Deng, J. Zhong, B. Wang, Q. Wang, Y. Xiao, J. Yuan, Risk factors influencing survival of acellular porcine corneal stroma in infectious keratitis: a prospective clinical study, J. Transl. Med. 17 (1) (2019) 434, https://doi.org/10.1186/s12967-019-02192-z.
[35] S. Mertsch, M. Hasenzahl, S. Reichl, G. Geerling, S. Schrader, Decellularized human corneal stromal cell sheet as a novel matrix for ocular surface reconstruction, Journal of tissue engineering and regenerative medicine 14 (9) (2020) 1318–1332, https://doi.org/10.1002/term.3103.
[36] K.H. Hussein, K.M. Park, Y.S. Lee, J.S. Woo, B.J. Kang, K.Y. Choi, K.S. Kang, H. M. Woo, New insights into the pros and cons of cross-linking decellularized bioartificial organs, Int. J. Artif. Organs 40 (4) (2017) 136–141, https://doi.org/10.5301/ojao.5000541.
[37] D. Pascolini, S.P. Mariotti, Global estimates of visual impairment: 2010, Br. J. Ophthalmol. 96 (5) (2012) 614–618, https://doi.org/10.1136/bjophthalmol-2011-300539.
[38] Q. Zheng, Y. Zhang, Y. Ren, Z. Zhao, S. Hua, J. Li, H. Wang, C. Ye, A.D. Kim, L. Wang, W. Chen, Deep anterior lamellar keratoplasty with cross-linked acellular porcine corneal stroma to manage fungal keratitis, Xenotransplantation 28 (2) (2021), e12655, https://doi.org/10.1111/xen.12655.
[39] H. Xu, J.S. Sapienza, Y. Jin, J. Lin, X. Zheng, H. Dong, H. Diao, Y. Zhao, J. Gao, J. Tang, X. Feng, D. Micceri, H. Zeng, D. Lin, Lamellar keratoplasty using acellular bioengineering cornea (BioCorneaVet(TM)) for the treatment of feline corneal sequestrum: a retrospective study of 62 eyes (2018-2021), animals : an open access, journal from MDPI 12 (8) (2022), https://doi.org/10.3390/ani12081016.
[40] J. Zhong, Y. Deng, B. Tian, B. Wang, Y. Sun, H. Huang, L. Chen, S. Ling, J. Yuan, Hyaluronate acid-dependent protection and enhanced corneal wound healing against oxidative damage in corneal epithelial cells, Journal of ophthalmology 2016 (2016), 6538051, https://doi.org/10.1155/2016/6538051.